Adsorption of Erythrosine-B on Mesoporous Graphitic Activated Carbon Prepared from Bael Tree (Aeglemarmelos) Bark: Equilibrium, Kinetics and Thermodynamic Studies.

S. Valliammai, Y. Subbareddy, K. S. Nagaraja, B. Jeyaraj

Department of Chemistry, Loyola Institute of Frontier Energy (LIFE),
Loyola College, Chennai, TN-600034, India.

Abstract

Mesoporous activated carbon was prepared from Bael tree bark (ACBTB) by impregnation with phosphoric acid at $450°C$. Materials were characterized for their surface chemistry by Boehm titrations, point of zero charge measurements, Fourier Transform Infrared spectroscopy (FTIR), thermogravimetric analysis (TGA), as well as for their porous and morphological structure by Scanning Electron Microscopy (SEM) and nitrogen adsorption at 77 K for the surface area. The effects of contact time, adsorbent dose, temperature, concentration and pH have been studied under batch system for Erythrosine-B (EB) dye. Adsorption isotherms were determined using Langmuir, Freundlich and Dubinin-Radushkevich models. The experimental data fitted best to the Langmuir model. The pseudo first order, pseudo second order and intra particle diffusion models were used to examine the kinetic data. The results obtained showed that kinetic data were well described by the second order model. Thermodynamic studies showed that the adsorption was spontaneous, endothermic and entropy controlled.

Keyword: Activated carbon, Porous, Adsorption, Isotherms, Kinetics, Thermodynamics.

1. Introduction.

Dyes and pigments have been extensively released in the wastewaters from different industries, particularly from textile, paper, rubber, plastic, leather, cosmetic, food, and drug industries. These dyes can cause allergic dermatitis, skin irritation, cancer and mutation in living organisms. It also causes eye burns, which may be responsible for permanent injury to the eyes of human and animals. On inhalation, it can give rise to short periods of rapid or difficult breathing, while ingestion through the mouth produces a burning sensation and may cause nausea, vomiting, profuse sweating, mental confusion, painful micturation, and methemoglobinemia –like syndromes [1]. There are more than 100,000 commercially available dyes with over 7 x 10^5 tones of dyestuffs produced annually [2].

Erythrosine is a water-soluble xanthenes class of dye. It is widely used as colorant in food, textile, drug and cosmetics. In large doses it causes various types of allergies, thyroid activities, carcinogenicity, DNA damage behaviour, neurotoxicity and xenoestrogen nature in the humans and animals. The photochemical and biochemical degradation of the erythrosine is not recommended due to formation of toxic by-products [3].

Many treatment methods have been adopted to remove dyes from wastewater, which can be divided into physical, chemical, and biological methods. Generally, physical methods which include coagulation [4], reverse osmosis [5], photo degradation [6], electrochemical oxidation [7], ion exchange, membrane filtration and adsorption [8] are effective for removing reactive dyes without producing unwanted by-products [9]. Adsorption is considered to be superior to other techniques because it is attributed to its low cost, easy availability, simplicity of design, high efficiency and ease of operation, biodegradability and ability to treat dyes in more concentrated forms [10].

A variety of adsorbents such as activated carbon, silica, bentonite, fuller's earth and alumina have been used for the removal of dyes from aqueous solutions. Among all these activated carbon is one of the most widely and popularly used adsorbent because of its high adsorptive capacity. Therefore low cost activated carbon has been widely used as an adsorbent [11] in surface chemistry [12] or separation process. But the main drawback is it is high cost and cannot be recycled. Hence some low cost adsorbents such as waste rice hulls [13], banana pith [14], rice straw [15], papaya seeds [16], neem leaves [17], De-oiled mustard [18], orange peels [19], bael tree bark [20] and seeds of *moringa olifera* [21] have been identified to be good sources of activated carbon which make them useful to be suitable precursors owing to their high-carbon and low-ash contents. Besides they are cheaper and readily available materials. In principle, preparation methods of activated carbon can be divided into two categories: physical activation and chemical activation. Compared with physical activation, chemical activation has the following advantages: low activation temperature, simple operation, and short activation time, low energy of consumption [22], higher yields, more surface area and better development of porous structures in carbon [23].

Bael tree is a spiny tree belonging to the family *rutaceae* and is abundantly found in India, Myanmar, Pakistan and Bangladesh [20]. The different parts of bael are used for various therapeutic purposes, such as for treatment of asthma, anemia, fractures, healing of wounds, swollen joints, high blood pressure, and jaundice. The major novelty of this work is the production of activated carbon by impregnation by chemical activation technique in a temperature of $450^{o}C$. In this study attempts have been made for the removal of Erythrosine-B from aqueous solution.

2. Materials and methods.

2.1. Chemicals and samples

Raw Bael tree bark was collected, washed many times with water and dried at room temperature. After grinding to fine powder, the mass was oven dried at $110^{o}C$. The dried mass was impregnated with orthophosphoric acid in the ratio of 5:1 (g H_3PO_4 /g Bael tree bark powder) and allowed to carbonize at $450^{o}C$ in a muffle furnace for 1h.The carbon so obtained was washed with distilled water to remove all the free acid until a constant pH was obtained and then dried at $110^{o}C$ overnight. Double distilled water was used for all the experimental studies.

 Erythrosine-B (EB) is an anionic dye with IUPAC name as Disodium 2-(2, 4, 5, 7-tetraiodo-6- oxido-3-oxo-3H-xanthen-9-yl) benzoate (Fig.1). The C.I. number of Erythrosine –B is 45430 and the λ_{max} is 526.Aqueous solution of the dye was prepared using double distilled water.
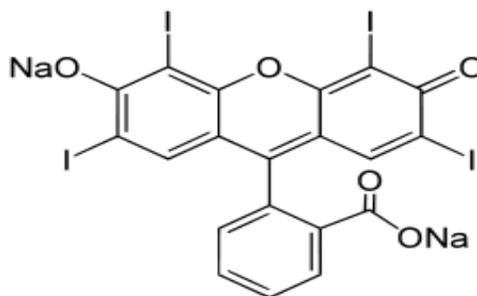
Figure1: Structure of Erythrosine-B

2.2. Characterisation of the adsorbent.

The mixtures were shaken using a shaker (Remi). The textural characterization of activated carbon of bael tree bark (ACBTB) was determined from N_2 adsorption – desorption isotherm at 77K using ASAP 2020 V3.01 G Micormeritics instrument. FT-IR spectra were recorded using MAGNA 550spectrophotometer. FEI Quanta FEG 200 High Resolution instrument was used for Scanning Electron Microscope images. The Raman spectrum was recorded by using BRUKER RFS 27: Stand alone FT-Raman Spectrometer. The thermal stability of ACBTB was studied with the help of TG/DTA using EX STAR 6300R, heating rate 10° min^{-1} in nitrogen

atmosphere. The percentage of C, H, N and O were analyzed by using FLASH EA 1112 series CHNS-O analyzer.

2.3. Batch and kinetic studies.

In order to evaluate the feasibility of adsorption, batch studies were carried out using 100ml conical flasks containing 50ml of the dye solution and a known amount of ACBTB adsorbent and then mechanically agitated in a water bath shaker (Remi) to elucidate the values of the test parameters including solution pH, dye concentration, temperature , contact time .These solutions were centrifuged at 5000rpm and the absorbance of the supernatant solution was determined at 526 nm by using a UV Visible spectrophotometer. The kinetic and thermodynamic studies were performed by determining removal conditions. The removal efficiency and adsorption by solid surface as adsorbents, q (mg/g) capacity were calculated with the following equation.

$$\text{Amount Adsorbed } (q_t) = (C_0 - C_t) \times \frac{V}{m} \qquad (1)$$

where C_0 and C_t (mol/L) are the concentrations of the dye solution initially and at time t respectively. V (L) is the volume of dye solution and m (g) is the mass of the adsorbent used.

2.4. Desorption studies.

The desorption studies were done to investigate the adsorption mechanism. Desorption experiments were conducted by taking 0.14g of ACBTB in 50ml of water, 0.1N HCl, 0.1N H_2SO_4, 0.1N CH_3COOH, 0.1N NaOH, CH_3COCH_3 and C_2H_5OH . The percentage of desorption of dye was obtained from the following equation.

$$\text{Percentage desorption} = \frac{\text{concentration of desorbed dye}}{\text{concentration of dye loaded on ACBTB}} \times 100 \qquad (2)$$

2.5. Testing of the real industrial effluent.

Experiment was carried out with the real effluent for the removal of dyes by using ACBTB. 50ml of the effluent was treated with 0.1g/L of ACBTB and subjected to shaking for 120 minutes at room temperature. The effluents before and after treatment were subjected to physical and chemical examination. To evaluate the toxicity of the adsorbed solutions, their initial and final COD [24] and BOD [25] values were determined as per standard methods.

3. Results and discussion.

3.1. Characterization of the ACBTB adsorbent.

3.1.1. Chemical Characterization of ACBTB by Boehm Titrations.

The Boehm titration method was used to determine the oxygen containing functional groups present over the surface of the activated carbon. 0.5g of the activated carbon (ACBTB) was kept in contact with 50ml of $NaHCO_3$(0.05N), Na_2CO_3(0.05N) and NaOH (0.05N)for acid groups and 0.05NHCl for basic groups respectively at room temperature for 24hr.Subsequently the aqueous solutions were back titrated with HCl (0.05N) for acidic groups and NaOH (0.05N)for basic groups. The acidic sites were calculated considering that NaOH neutralizes carboxylic, lactones and phenolic groups, Na_2CO_3 neutralizes carboxylic and lactone groups and $NaHCO_3$ neutralizes carboxylic groups only. The difference in the titration value of Na_2CO_3 and $NaHCO_3$ was due to lactone and the difference in the titration value of NaOH and $Na_2CO_3$was assumed to be phenol. Basic sites were determined by titration with HCl.The most common oxygen groups on the surface are carboxylic (0.41meq/g), phenolic (0.442meq/g), lactonic (0.1meq/g) and basic sites (0.145meq/g).

3.1.2. Textural characterization of ACBTB.

Surface area is one of the most important properties of adsorbents. Table.1 represents the textural charaterisation of ACBTB. The surface area of ACBTB was 804.18 m²/g which is much higher than the wood based activated carbon (769 m²/g) and coal - based activated carbon (331 m²/g) [26]. According to the classification adopted by IUPAC, adsorbent pores are classified into three groups: micropore (diameter < 2 nm), mesopore (2-50 nm) and macropore (>50 nm). The BJH pore size distribution measurement indicates that the

sample has mesoporosity with pore diameter in the range of 5 – 40 nm. The average pore diameter of ACBTB was found to be 5.54 nm (Table 1) which further indicated that ACBTB was mesoporous.

Table1: S_{BET} and pore structure of ACBTB.

S_{BET} (m^2/g)	S_{ext} (m^2/g)	S_{ext}/S_{BET} (%)	S_{mic} (m^2/g)	S_{mic}/S_{BET} (%)	V_{tot} (cm^3/g)	V_{mic} (cm^3/g)	V_{meso} (cm^3/g)	D_p (nm)
804.18	665.04	82.70	139.13	17.30	1.114	0.060	1.05	5.54

3.1.3 .Scanning electron microscopy images.

The Scanning electron microscopy images of the adsorbent (ACBTB) before the adsorption is shown in Fig.2.The surface morphology of the activated carbon observed by SEM indicates that the activated carbon has different sizes of cavities. This might be due to the presence of mesoporous nature of activated carbon. These pores are enough for the sufficient adsorption of the dye molecules into them. The chemical composition of ACBTB was determined using CHNS analyser.The results showed that the major constituent was carbon(62.27%), along with some amount of oxygen(18.01%),hydrogen(2.92%) and nitrogen(1.79%).
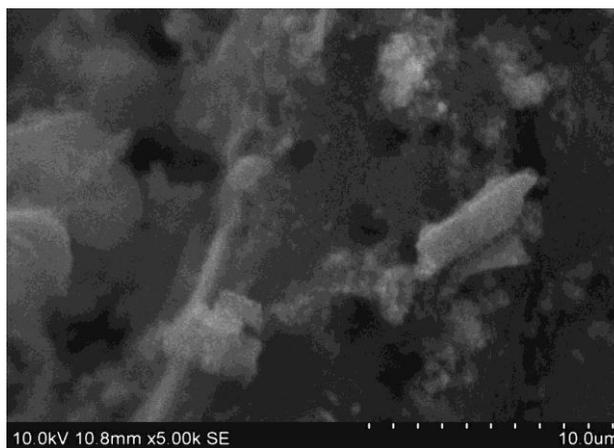
Figure 2: SEM image of ACBTB before adsorption.

3.1.4. FT-IR analysis

The broad peak at 3397.4 cm^{-1} is due to the O-H stretching vibration mode of the hydrogen bonded hydroxyl functional group due to moisture and from carboxyls, phenols or alcohols [27]. The location of the hydrogen bonded OH group is usually in the range of 3200- 3650 cm^{-1} for alcohols and phenols. The band located at 2360.6 cm^{-1} is due to the attribution of C= C stretching [22].The peak at 1695.8 cm^{-1} refers to the symmetric stretching mode of C= O in the carboxylic acid group (COOH stretching) [28] or v(C=O) vibrations in carboxylate groups [29]. The spectra of ACBTB shows a strong band at 1585 cm^{-1} which could be attributed to the carbonyl stretching vibration of carboxylic acids, lactones [30] (Fig.3). The FTIR spectrum gave a supported evidence for the presence of surface groups as estimated by Boehm titrations.

After the dye adsorption the peaks at 3397.19 cm^{-1}, 2360.6 cm^{-1}1695.8 cm^{-1}and 1585 cm^{-1}(Fig.3) are found to shift to the wavelengths of 3407.4 cm^{-1}, 2359 cm^{-1},62359 cm^{-1} and 2108 cm^{-1} respectively confirming that OH and C=O groups are involved in the adsorption process of Erythrosine-B on ACBTB.

3.1.5 XRD-analysis.

The X-ray diffraction pattern of the activated carbon exhibited two peaks at 2θ = 25.6 and 43.069 (Fig.4) which are similar to that of graphite [31]. The crystallite size of ACBTB along L_c or L_a was determined by Scherer equation [32]:

$$L_{c(a)} = \frac{K_{c(a)}\lambda}{\beta_{c(a)}\cos\theta c_{(a)}} \qquad (3)$$

Where β is the full width at half maximum of the lines and λ is the X-ray wavelength. The shape factor $K_{c(a)}$ is equal to 0.94 and 1.84 for L_c and L_a respectively.
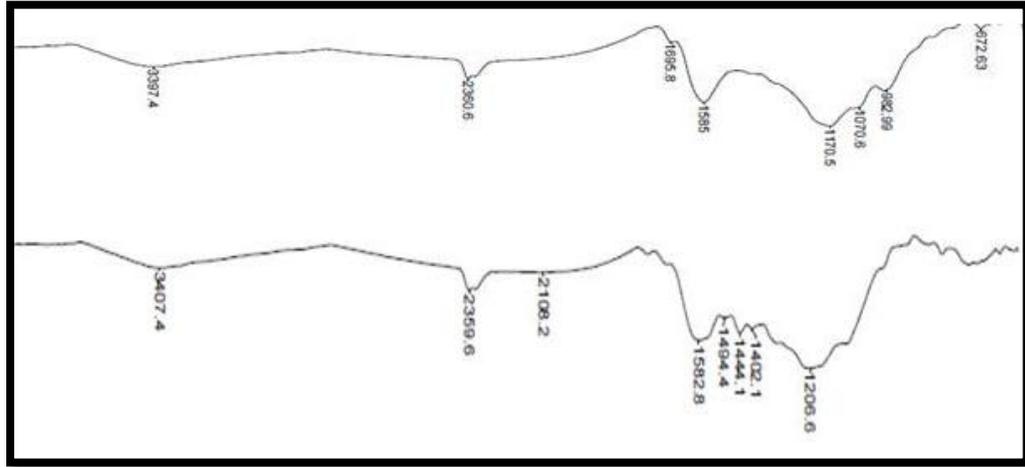
Figure3: FTIR analysis of ACBTB before and after adsorption.

The peaks obtained at $2\theta = 25.60$ and 43.06 which are attributed to (002) plane and (101) plane respectively are used to calculate the values of L_c and L_a [32]and the values are 2.955nm and 6.009nm respectively. The interlayer spacing (d_{002}) was calculated using Bragg's equation. Typically, in a crystalline carbonaceous structure, such as graphite, the interlayer distance between two adjacent carbon sheets is0.335 nm. In this study, the peak at $2\theta = 25.60°$corresponds to an interlayer distance of 0.386 nm, which is quite near to that of pure graphitic carbon[33].It is predominantly seen that the activated carbon is graphitic in nature.
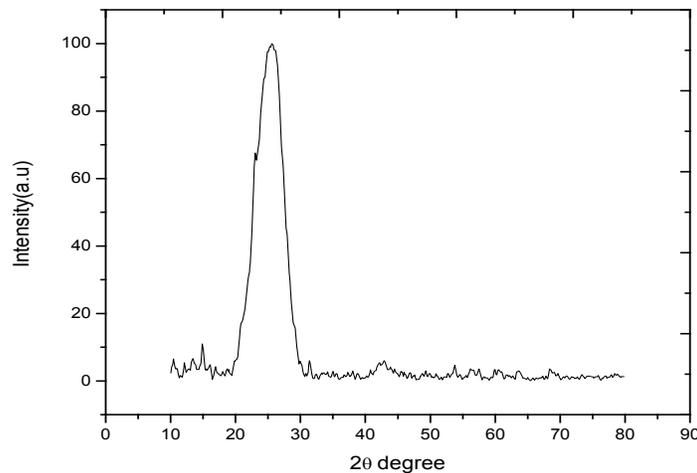
Figure4:X-Ray diffraction pattern of ACBTB.

3.1.6. Raman Spectroscopy.

   Information on the crystallographic disorders in carbons can be obtained by Raman spectroscopy. The graphitic characteristic of ACBTB is further confirmed by Raman spectroscopy. The material exhibited two

distinct peaks (Fig.5) at about 1350 cm^{-1} (D-band) and 1591 cm^{-1} (G-band) [34]. In addition, a peak at 2707 cm^{-1} (2D-band) was clearly observed in ACBTB, which can be observed only in highly-developed graphitic carbon .The G-band is related to the vibration of sp2 bonded carbon atoms in a two-dimensional hexagonal lattice, which often relates to the formation of ordered graphite layers. The D-band is often referred to the "disorder" band, which results from the imperfection or loss of hexagonal symmetry of the graphite structure. It is known that the relative intensity ratio between the D and G bands (ID/IG) reflects the degree of graphitization. Accordingly, the low ID/IG value indicates a high degree of graphitization [35].The ID/IG value of ACBTB is 0.8485, suggesting that the ACBTB has highly graphitic characteristic with high degree of graphite ordering. The above mentioned bands and the value of ID/IG confirm the presence of graphitic carbon in the ACBTB.
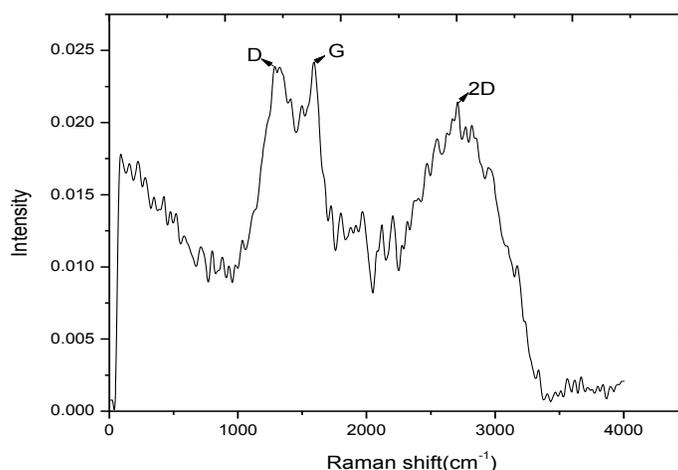
Figure5: Raman spectra of ACBTB.

3.1.7. Thermal stability of ACBTB

The results of thermo gravimetric analysis (TG) carried out for ACBTB infers that the decomposition occurs in three stages (Fig.6).The first stage in the temperatures range 35 to 65°C involves the loss of moisture with a weight loss of 20% [36].ACBTB was found be thermally stable in the temperature range of 100-550°C which indicates that 450°C can be chosen for the preparation of the adsorbent. The maximum rate of weight loss occurred at the third stage approximately with a weight loss of 75%.
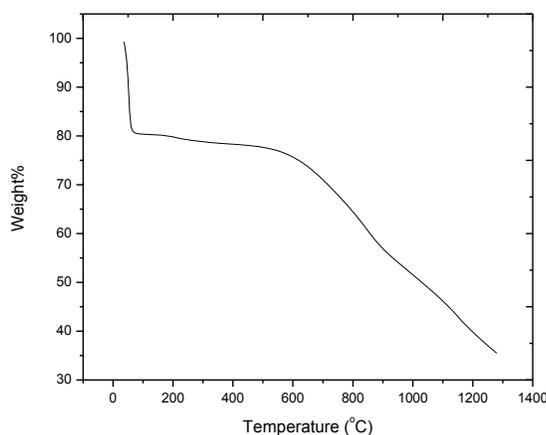
Figure 6: TG curve of activated carbon (ACBTB), 2hrs duration time at 450°C.

3.1.8. Zero point charge of ACBTB

The point of zero charge of ACBTB was determined by solid addition method. In this method 0.1M KCl solution was taken in ten bottles maintained with pH in the range of 1-10 and 0.1g of ACBTB was added to each .These solutions were shaken for 24h at room temperature and the final pH was measured. The difference between the initial and final pH was measured and the point where $\Delta pH = 0$ was taken as the point of zero charge [37]. At pH<pHzpc, the surface has a net positive charge and at pH > pHzpc, it is negative. The pHzpc of ACBTB was found to be 2.2. This type of low value was reported for the activated carbon from coir pith as an agricultural solid waste [38].

3.2. Effect of adsorbent mass.

The effect of adsorbent mass quantity on the removal of the dye is shown in Fig.7. The percentage of the dye adsorbed increased from 22.24% to 99.40% by increasing the mass of adsorbent. The adsorbent efficiency increased by increasing the adsorbent mass from 0.04g to 0.32g and reached the equilibrium at a dosage of 0.14g of ACBTB. An increase in the adsorption may be concluded due to the increase in the adsorbent surface and therefore more active functional groups resulting in the availability of more adsorption sites [27].
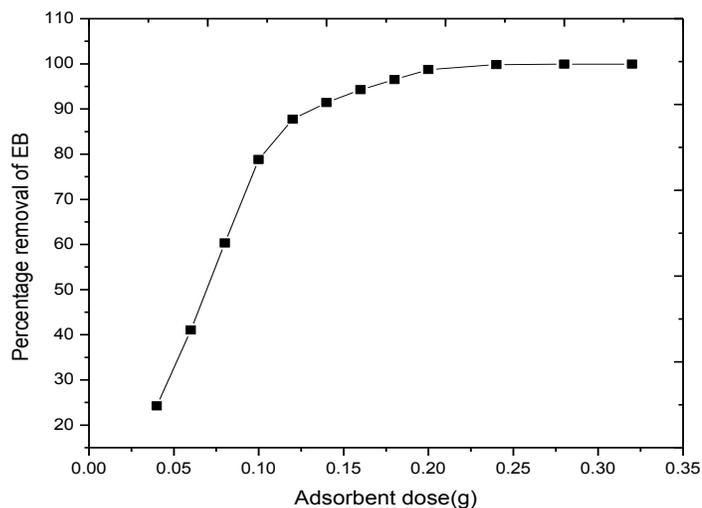
Figure7: Effect of adsorbent dose on uptake of EB by ACBTB

3.3. Effect of contact time.

The effect of contact time on the adsorption of EB was studied (Fig.8) for different concentrations. The adsorption experiments were carried out under a regular interval of time with a fixed adsorbent dose of 0.14g.The contact time needed for EB solutions with initial concentrations of 1.2×10^{-3}, 1.4×10^{-3} and 1.8×10^{-3} M in reaching the equilibrium was about 120 min. The optimum contact time is found to be 120 min to study the other parameters.

3.4. Effect of concentration at different temperature

The adsorption of EB was recorded in the concentration range from 0.4×10^{-3} M to 2.0×10^{-3} M at fixed dose of 0.14g ACBTB in the temperature ranges at 305, 315 and 325 K(Fig .9). It is observed that the adsorption of EB increased with increasing temperature. This may be due to the increasing mobility of the dye molecule and an increase in the number of active sites for the adsorption [6].The positive effect of temperature on the adsorption of EB indicates that the process is endothermic in nature.

Valliammai et al.
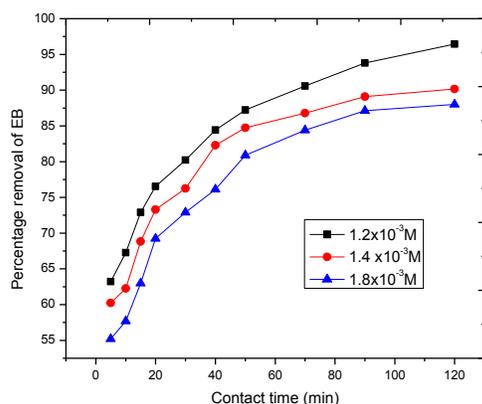
Figure 8: Effect of contact time for the removal of EB at different concentrations using ACBTB.
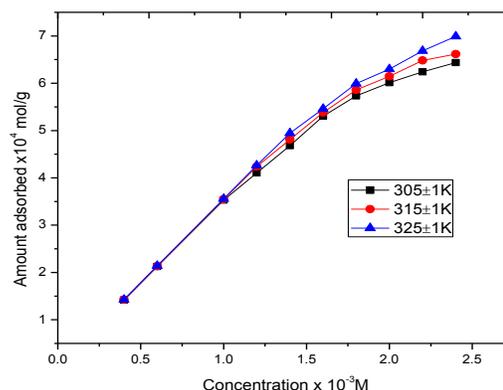
Figure 9: Effect of temperature on the uptake of EB at different concentrations.

3.5. Effect of pH

The pH of a medium will control the magnitude of electrostatic charges which are imparted by the ionized dye molecules as a result the rate of adsorption will vary with the pH of an aqueous medium. The effect of pH was studied with a fixed adsorbent dose of 0.14g with a dye concentration as 1.8×10^{-3} M and varying the pH by adding 0.1N of NaOH or HCl solutions and then shaked until equilibrium reached. When the pH was increased (Fig.10) from 2 to 12 the adsorption of EB decreased from 99.75 to 57.49 %.This can be explained in terms of pHzpc. The pHzpc of ACBTB was found to be 2.2. At pH <pHzpc the surface of ACBTB is positively charged and the electrostatic attraction between negative adsorbate ions and adsorbate particles helped to increase the adsorption capacity of Erythrosine–B. The lower the pH of the solution the higher the removal efficiency. At pH >pHzpc the adsorbent surface is negatively charged, the electrostatic repulsive force between the negative adsorbate ions and the negative adsorbent particles would decrease the adsorption capacity of Erythrosine –B [22].
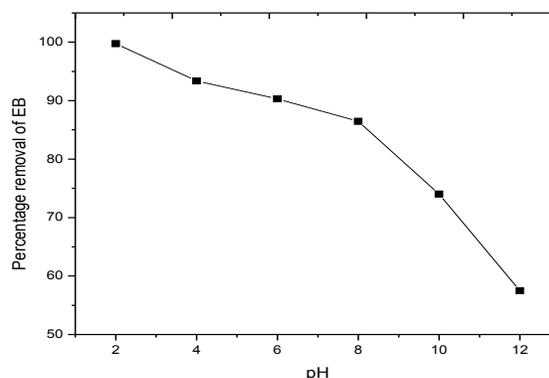
Figure 10: Effect of pH on the removal of EB onto ACBTB at contact time 120min with ACBTB.

3.6. Adsorption Isotherm

The relation between the amount of the substance adsorbed at constant temperature and its concentration in equilibrium solution is called the adsorption isotherm. Generally, adsorption isotherms are used to determine the adsorption capacity of adsorbent at particular temperature and to optimize the design of an adsorption system. Equilibrium isotherm equations are used to describe the experimental adsorption data. The parameters obtained from the different models provide important information on the adsorption mechanism and

the surface properties and affinities of the adsorbent [39].Three adsorption isotherms, Langmuir, Freundlich and Dubinin- Radushkevich were employed to analyze the experimental adsorption data.

3.6.1. Langmuir adsorption isotherm

Langmuir isotherm was chosen for the estimation of the maximum adsorption capacity corresponding to complete mono layer coverage on the adsorbent surface. The Langmuir linear form of the equation is [40]

$$\frac{C_e}{q_e} = \frac{1}{Q_m K_L} + \frac{1}{Q_m}C_e \qquad (4)$$

where, q_e(mol/g) and C_e(mol/L) are the amount of dye adsorbed per unit weight of adsorbent and the concentration of the dye solution at equilibrium respectively. The constant Q_m(mol/g) is the adsorption capacity and K_L (L/mol) is the Langmuir equilibrium constant. Therefore, a plot of C_e/q_e versus $C_e$gives a straight line of slope $1/Q_m$with intercept$1/Q_m K_L$ (Fig.11). The feasibility of Langmuir adsorption isotherm was tested by using the following equation [41].

$$R_L = \frac{1}{1 + K_L C_0} \qquad (5)$$

where C_0 is the initial dye concentration (mol/L) and K_L (L/mol)is Langmuir equilibrium constant. The value of R_L indicates the type of adsorption isotherm to be unfavorable ($R_L > 1$), linear ($R_L = 1$), favorable ($0 < R_L < 1$) or irreversible ($R_L = 0$) [10].

The correlation coefficients reported in Table 2 show that the adsorption of EB onto ACBTB follows Langmuir adsorption. R_L values for the removal of EB lie between 0.023 and 0.050 which indicates favorable adsorption. The maximum monolayer adsorption capacity of EB is 576.12 mg/g (6.5479 x 10^{-4}mol/g).The adsorption capacity is found to higher than that of other activated carbon.
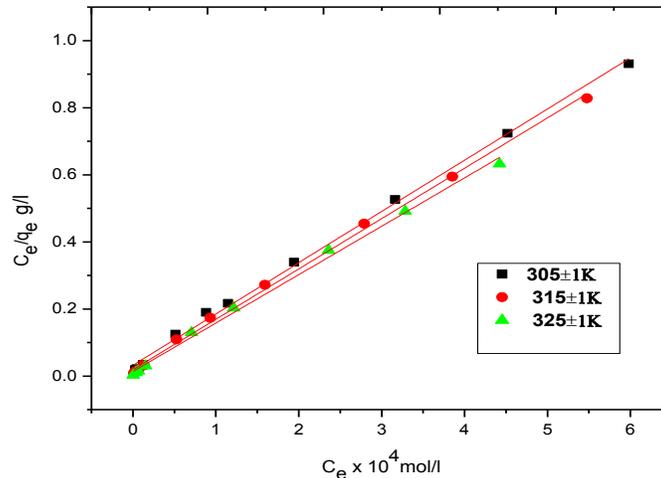
Figure 11: Langmuir adsorption isotherm of EB onto ACBTB at different temperatures.

3.6.2. Freundlich adsorption isotherm

The Freundlich isotherm model is the earliest known equation describing the adsorption process. It is an empirical equation [42] and can be used for the assumption of heterogeneous adsorption. The applicability of the Freundlich adsorption isotherm was also analyzed (Fig .12) using the same set of experimental data by plotting log (q_e) versus log (C_e).

$$\log(q_e) = \log(K_f) + \frac{1}{n}\log(C_e) \qquad (6)$$

K_f (mol/g) and n are the Freundlich constants, indicating adsorption capacity and adsorption intensity respectively. If n values are between 1 to 10 then it represents the best adsorption [10].Table 2shows that the Q_m

and K_f values increase with increasing temperature indicating the adsorption is endothermic in nature and the n value is between 7 and 9, favouring adsorption of EB onto ACBTB.
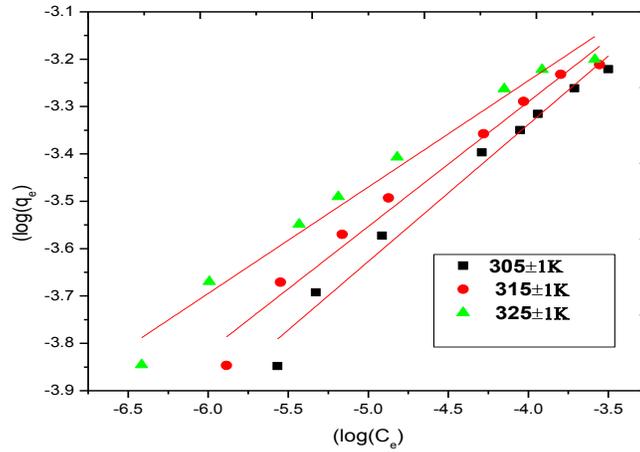
Figure 12: Freundlich adsorption isotherm for adsorption of EB by ACBTB.

3.6.3. Dubinin-Radushkevich (D-R) adsorption isotherm

Dubinin–Radushkevich (D–R) isotherm is used to distinguish whether the adsorption takes place by physical or chemical processes. It describes the adsorption on both homogeneous and heterogeneous surfaces. The linear form of the isotherm can be expressed as follows [43]:

$$\ln(q_e) = \ln(Q_m) - K\varepsilon^2 \qquad\qquad (7)$$

where K is constant related to the adsorption constant (mol^2/kJ^2), and ε is the Polanyi potential that can be calculated from the equation [44].

$$\varepsilon = RT \ln\left(1 + \frac{1}{C_e}\right) \qquad\qquad (8)$$

where R is the Universal gas constant $(8.314\ Jmol^{-1}K^{-1})$, T is the temperature (K) and C_e is the concentration at equilibrium. Fig .13 shows the plot of ln (q_e) vs ε^2 of the experimental data for the adsorption of EB onto ACBTB. The slope gives K and from the intercept the adsorption capacity Q_m can be calculated.
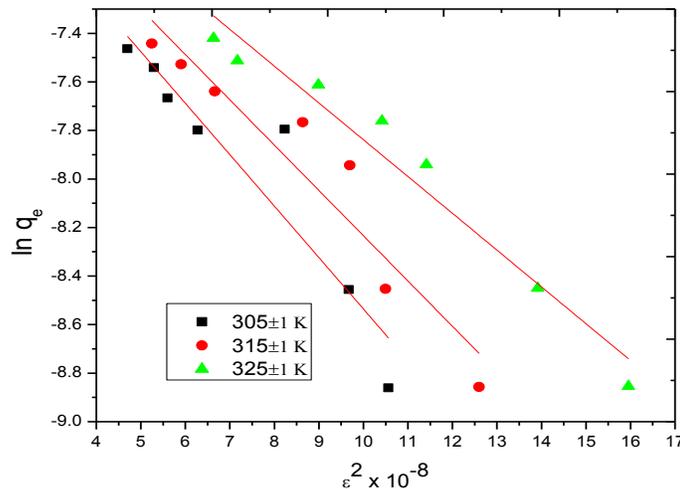
Figure 13: D-R isotherm plots for the adsorption of EB on ACBTB.

The mean energy of sorption, *E* (kJ/mol), is calculated by the following equation:

$$E = \frac{1}{\sqrt{(2K)}} \qquad (9)$$

The mean sorption energy (E) calculated from D-R isotherm provides important information about the physical and chemical nature of the adsorption process. The mean energy of adsorption (E) values was in the range of 15.35 to18.16kJ/mol for EB indicating the adsorption takes place by chemisorption.

Among the various isotherm plots it is seen that the Langmuir equation gave best fit suggesting monolayer chemisorption of EB on the surface of ACBTB because the R^2 values are comparatively higher than that of the other isotherms(Table.2).

Table 2: Adsorption isotherm parameters for the adsorption of EB onto ACBTB

Adsorption isotherms	305	315	325
Langmuir isotherm			
Qm(mol/g)	6.5479×10^{-4}	6.6613×10^{-4}	6.9290×10^{-4}
K_L(1/mol)	4.7106×10^{4}	7.9050×10^{4}	10.6195×10^{4}
R^2	0.996	0.998	0.998
R_L	0.0503	0.0306	0.0230
Freundlich isotherm			
K_f(mol/g)	1.466×10^{-3}	1.818×10^{-3}	2.012×10^{-3}
1/n	0.111	0.131	0.136
n	9.004	7.621	7.346
R^2	0.978	0.976	0.975
D-R isotherm			
Qm(mol/g)	1.6342×10^{-3}	1.7155×10^{-3}	1.7953×10^{-3}
K	2.1194×10^{-9}	1.8658×10^{-9}	1.5159×10^{-9}
R^2	0.861	0.891	0.950
E	15.359	16.370	18.161

3.7. Adsorption kinetics.

The rate constant for the adsorption of EB was determined using pseudo first order, pseudo second order and intra particle diffusion models.

3.7.1 Pseudo first order equation.

The adsorption kinetic data were described by the Laregren pseudo first order model which is the earliest known equation, describing the adsorption rate based on the adsorption capacity. The pseudo first order rate equation can be written as [45].

$$\log(q_e - q_t) = \log q_e - \frac{k_1}{2.303}t \qquad (10)$$

where q_e and q_t (mol/g) are the amounts adsorbed at equilibrium and at a time t and k_1 is the rate constant of the pseudo first order adsorption and presented in Fig.14. The correlation coefficients are found to be high but the q_e calculated values are not in coincidence with the q_e experimental values. Hence adsorption does not follow to the pseudo first order model.

3.7.2. Pseudo second order equation

The adsorption kinetic may be described by the pseudo second order rate model [46].

$$\frac{t}{q_t} = \frac{1}{k_2 q_e^2} + \frac{1}{q_e}t \qquad (11)$$

where k_2 is the rate constant of the pseudo second order adsorption (g mol^{-1}min^{-1}).

The values of the various parameters (q_e, k_1 and k_2) were calculated by using the intercept and the slope obtained from the plots and tabulated in Table 3.Fig.15 shows the plot of second order (t/q$_t$vs t) kinetic model. The values of R^2 are closer to unity in pseudo second order (0.998) than in the pseudo first order. The values of q_e calculated from pseudo second order are in good agreement with q_e experimental values and this indicates that the adsorption system obeys the pseudo second order kinetic model
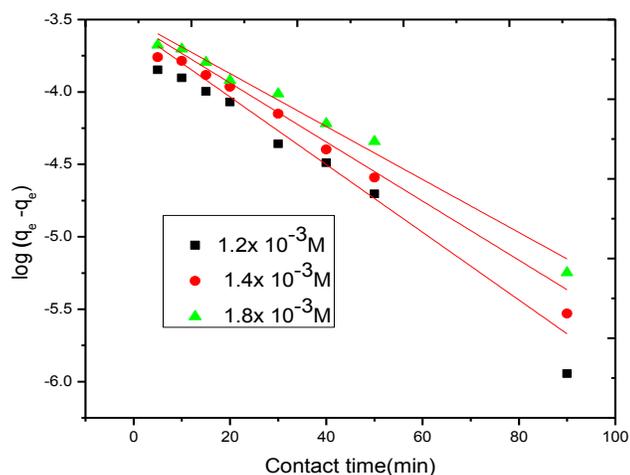
Figure 14: Pseudo first order kinetic plot for the adsorption of EB on ACBTB.
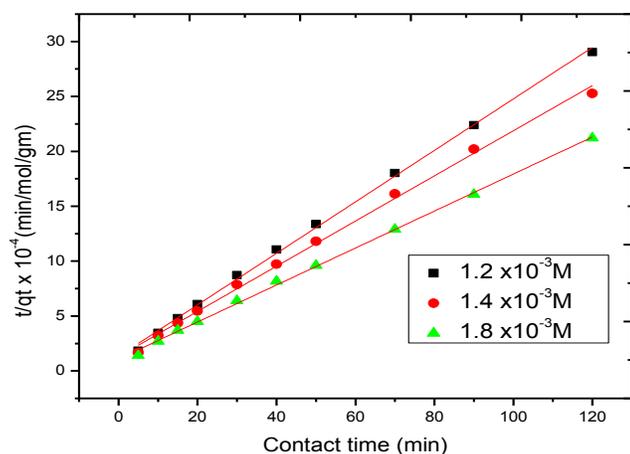
Figure15: Pseudo second order kinetic plot for the adsorption of EB on ACBTB.

Table 3: Adsorption kinetic parameters for the adsorption of EB by ACBTB.

Adsorbate con(M)	q_e(exp) (mol/g)	Pseudo first order			Pseudo second order			
		k_1 (1/min)	q_e (mol/g)	R^2	k_2 (g/mol min)	q_e (mol/g)	h (mol/g/min)	R^2
12 x 10^{-4}	4.1334x10^{-4}	0.0538	2.7131x10^{-4}	0.992	0.413x10^3	4.264x10^{-4}	7.518x10^{-4}	0.998
14 x 10^{-4}	4.7497x10^{-4}	0.0468	2.9533x10^{-4}	0.966	0.3228x10^3	4.8614x10^{-4}	7.6288x10^{-4}	0.998
18 x 10^{-4}	5.6571x10^{-4}	0.0421	3.1149x10^{-4}	0.948	0.261x10^3	5.935x10^{-4}	9.214x10^{-4}	0.988

3.7.3. Intra-particle diffusion model.

The possibility of intraparticle diffusion was explored by using intraparticle diffusion model, which is commonly expressed by the following equation:

$$q_t = k_{id}t^{1/2} + C \qquad (12)$$

where k_{id} (molg^{-1}min$^{-1/2}$) is the intraparticle diffusion rate constant, C is the intercept, which is related to thickness of the boundary layer. k_{id} and C can be obtained from the slope and intercept of q_t versus $t^{1/2}$.

Fig.16 shows the plot of intra particle diffusion of EB onto ACBTB. The data showed a multi linear plot which indicates that two or more steps influence the sorption process. The first linear trend is due to the diffusion of adsorbate through the solution to the external surface of the adsorbent or boundary layer diffusion of solute molecules. Second linear portion indicates the gradual reach of equilibrium stage and the third is due to the low adsorbate concentration left in the solution [7]. The slope of the first linear portion gives the intra-particle rate constant (k_{id}) and the intercept of this portion is proportional to the thickness of boundary layer [47]. The lines do not pass through the origin and therefore intra-particle diffusion is not the rate determining step and boundary layer control may be involved in the process. From Table 4 it was observed that the values of C increased with the increase in the concentration of the EB, which indicated an increase in the thickness and the effect of the boundary thickness [10].
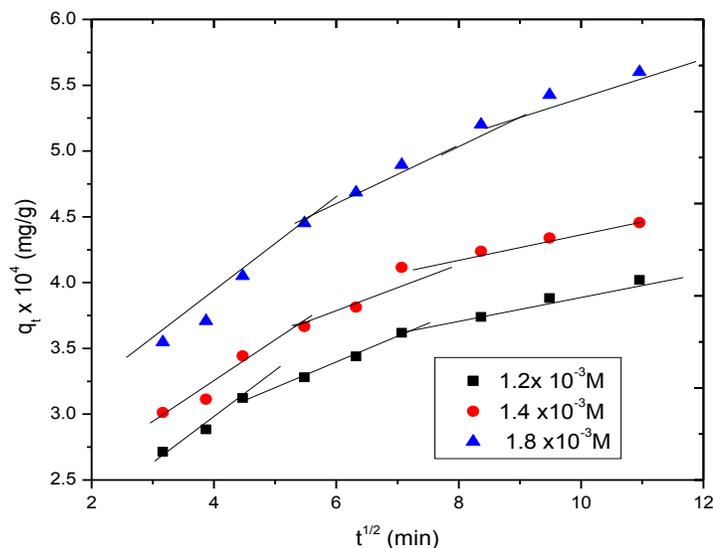
Figure 16: Intra-particle diffusion plot for the removal of EB by ACBTB.

Table 4: Intra – particle diffusion for the adsorption of EB by ACBTB.

Intra-particle diffusion constants			
Adsorbate conc (M)	**k_{id}(molg^{-1}min$^{-1/2}$)**	**C(mol/g)**	**R^2**
1.2 x 10^{-3}	0.252x 10^{-4}	1.929x10^{-4}	0.953
1.4 x 10^{-3}	0.299x 10^{-4}	2.035x1^{-4}	0.933
1.8 x 10^{-3}	0.4046x 10^{-4}	2.221x10^{-4}	0.971

3.8. Thermodynamic parameter

The thermodynamic parameters such as Gibbs free energy change (ΔG°), enthalpy change (ΔH°), and entropy change (ΔS°) of the system were calculated from the Langmuir isotherms using the equations 13 to 15. Thermodynamic parameters determine the spontaneity and the nature of the adsorption process:

$$\Delta G^0 = -RT \ln K_L \tag{13}$$

$$\Delta H^0 = -R \frac{T_2 T_1}{T_2 - T_1} ln \frac{K_{L2}}{K_{L1}} \tag{14}$$

$$\Delta S^0 = \frac{\Delta H^0 - \Delta G^0}{T} \tag{15}$$

where K_L , K_{L1} , K_{L2} (L/mol) are the Langmuir equilibrium constants at 305,315 and 325 K respectively and obtained from the plot of C_e/q_e versus C_e, and R ($8.314 Jmol^{-1}K^{-1}$) is universal gas constant.

The negative values of ΔG^0 (-27.28 to -31.27kJ/mol) confirm the feasibility and spontaneous nature of the adsorption process. ΔH^0 and ΔS^0 were calculated and the values are found to be 25.125 kJ/mol and171.83 J/molK respectively. The positive value of enthalpy change (ΔH^0) further accounts for the endothermic nature, while positive ΔS^0 value reflects that the adsorption mechanism is an entropy controlled process. Even though the positive value of ΔH^0 indicates the endothermic process, the process becomes spontaneous having negative value of ΔG^0 because of the positive value of ΔS^0.

4.0 Comparison of adsorption capacity of ACBTB with other low cost adsorbent.

Table 5 shows a comparison of maximum adsorption capacities of different low cost adsorbents and activated carbons used for removal of dyes. The adsorption capacity of ACBTB obtained in this study (576.12 mgg^{-1}) is much higher than that of other low-cost adsorbents.

Table 5: Adsorption capacity of various adsorbents

Adsorbent	Maximum adsorption capacity (mgg^{-1})	References
Pitch pine sawdust	20.8	[1]
Wheat shells	16.56	[1]
Coffee husks	90.09	[37]
Coir pith carbon	5.87	[37]
Peanut hull	68.03	[48]
Banana Peel	20.8	[48]
Orange peel	27.78	[49]
Maize cob carbon	233.40	[50]
Bamboo dust carbon	7.20	[51]
Groundnut shell carbon	7.50	[51]
Rice husk carbon	37.57	[51]
Coconut shell carbon	8.16	[51]
Bael tree bark carbon	**576.12**	**Present study**

5.0 Desorption studies.

The desorption studies are necessary to elucidate the nature of adsorption mechanism and to regenerate the adsorbent. It has been reported that, if the adsorbed dye on the solid surface can be desorbed by water, the attachment of the dye on the adsorbent is by weak bonds. If alkali is needed, then the adsorption is by ion exchange [52]. If organic solvents (CH_3COOH, C_2H_5OH) can desorb the dye then adsorption is chemisorption [53].Water, 0.1N HCl, 0.1N H_2SO_4, 0.1N CH_3COOH, 0.1N NaOH, CH_3COCH_3 and C_2H_5OH were used to recover the adsorbent.

The percentage of desorption by water, HCl and NaOH are 2.87% and 0.98 respectively. When acetic acid, ethanol and acetone were used, it led to thedesorption of 43.8%, 45.53% and 54.29% respectively. The maximum desorption occurred with acetone as the desorbing medium.

6.0 Testing of real effluent by using ACBTB

To evaluate the efficiency of the prepared adsorbent ACBTB towards the removal of the dyes, the real effluent collected from a textile industry was used. The absorbance was found for the real effluent before carrying out the experiment. The adsorption of the dyes was performed by adding 0.1g/L of ACBTB to 50ml of the real effluent and subjected to shaking for 120 minutes. These solutions were then filtered and the absorbance was measured. Fig.17 shows the absorbance in the whole range of the visible spectrum for the textile effluent before and after the addition of ACBTB.The treated solution the real effluent was tested for various physical and chemical parameters. The result of the physical examination showed that there was a complete decolourisation, removal of odour and decrease in the turbidity level (36 to 1.6 NTU). Chemical examination result showed that the COD value decreased from 6060 mg/L to 733 mg/L and that of BOD from 1800 mg/L to 250 mg/L
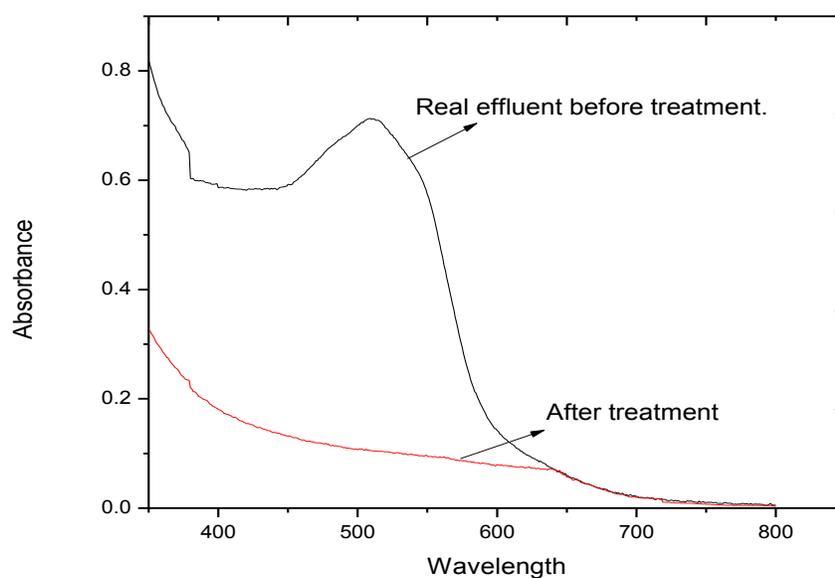
.**Figure 17:** Spectra of the real textile effluent before and after treatment with ACBTB

Conclusions

1. The results of present investigation show that the activated carbon of Bael tree (*Aeglemarmelos*) bark (ACBTB) can be used as an effective adsorbent for the removal of Erythrosine-B from aqueous solutions and is an alternative to the expensive materials available in the market.
2. The adsorption of the dye was found to increase with increase in adsorbent dose, contact time and temperature and decrease with increase in pH (2-12).
3. Equilibrium data best fitted to the Langmuir adsorption isotherm, which confirmed the monolayer adsorption of EB onto ACBTB with a monolayer adsorption capacity of 6.5479×10^{-4}mol/g.
4. The adsorption kinetics of EB with ACBTB followed pseudo second order because the values of calculated q_e and experimental q_e were equal.
5. The positive value of $\Delta H°$ indicates that the adsorption of EB over ACBTB is an endothermic process. The negative value of $\Delta G°$ indicates the spontaneous nature of the adsorption process and is entropy driven process.
6. The results of the physical and chemical examination of the textile effluent after treatment with ACBTB showed that there was a complete decolourisation, removal of odour, decrease in turbidity, COD and BOD levels.
7. ACBTB can be utilized as a low cost and efficient absorbent for the removal of EB from aqueous solutions and it has the potential to be used for treatment of real effluents.

References

1. Hameed B.H., Mahamoud D.K., Ahmad A.L., *J. Hazard. Mater*.158 (2008) 65.
2. Sonawane G.H., Shrivastava, V.S., *Desalination.* 247 (2009) 430.
3. Mittal A., Mittal J., Kurup, L., Singh A.K., *J. Hazard. Mater*. 138 (2006) 95.
4. Kannan C., Bhuvaneswari N., Palvannan T., *Desalination.* 249 (2009) 1132.
5. Wu H.,   Xie Y., Zhao J., Hidaka H., *J. Mol. Catal,A: Chem.* 144 (1999) 77.
6. Mittal A., Mittal, J., Malviya, A., Kaur, D., Gupta, V.K., *J.Colloid Interface Sci*. 342 (2010) 518
7. Mane V.S., Vijay P.V., *Desalination.* 273 (2011) 321.
8. Chuah T.G., Jumasiah A., Azni I., Katayon S., Thomas Choong S.Y., *Desalination*.175 (2005) 306.
9. Al-Degs Y.S., El-Barghouthi M. I., El-Sheikh A.H., Walker G. M., *Dyes and Pigments.* 77 (2008)   17.
10. Bulut Y., Aydin H., *Desalination.* 194 (2006) 260.
11. Kumar P.S., Ramalingam S., Sathishkumar K., *Korean*. *J. Chem. Eng.* 28(2011)149.
12. Wang S., Zhu Z.H., *Dyes and Pigments*. 75 (2007) 306.
13. Daniel G., de Luna., Edgar D., Flores., Angela D., Genuino., Cybelle M., Futalan., Meng-Wei Wan., *J.Taiwan Inst Chem Eng.* 44 (2013) 646.
14. Namasivaya, C., Prabh, D., Kumuth, M., *Bioresour Technol*. 64 (1998) 77.
15. Gong R., Jin Y., Chen F., Jian Chen., Zhili Liu., *J. Hazard. Mater.* 137 (2006) 865.
16. CarolineT.W. , Gabriela C. C., Marcio A.M. , Foletto E.L., Dotto G.L., *Water sci. Technol.* 70 (2014) 102.
17. Kornwipha S., Nittaya W., Ratchaneekorn W., *International Journal of Scientific and Research Publications.* 4 (2014) 1.
18. Jain R., Sikarwar S., *J.Hazard. Mater.* 164 (2009) 627.
19. Kumar V.K., Porkodi K., *Dyes and Pigments.* 74 (2007) 590.
20. Valliammai S., Subbareddy Y., Nagaraja K.S., Jeyaraj B., *International Journal of Green and herbal chemistry.* 2(2013) 975.
21. Marandi R., Sepehr S.M.B., *American Journal of Environmental Engineering.* 1(2011) 1.
22. Xiao H., Peng H., Dend S., Yang X., Zhang, Y., Li Y., *Bioresour Technol*.111 (2012) 127.
23. Sugumarn P., Priya V., Ravichandran P., Seshadri S., *Journal of Sustainable Energy & Environment.* 3 (2012) 125.
 24. Hur J., Lee B., Lee T., Park D., *Sensors* 10 (2010) 2462.
 25. Dogar N., Nawaz M., Majeed M., Saeed A., *Journal of Scientific and Innovative Research* 2 (2013) 355.
26. Wang L., Zhang J., Zhao R., Li C., Li Ye., Zhang C., *Desalination*. 254 (2010) 69.
27. Rasool M. M., Hosseini S., Yazdi S.K., Soltani S.M., Rahim M. M., *Chem. Eng. Res. Des*. 90 (2012) 707.
 28. Jadhav D.N., Vanjara A.K., *Indian J.Chem Tech*nol. 11 (2004) 195.
29. Yang T., ChongLua A., *J.Colloid Interface Sci.* 267 (2003) 413.
30. Liu H., Wang X., Zhai G., Zhang J., Zhang C., Bao N., Cheng C., *Chem. Eng.J.* 209 (2012) 159.
31. SathishKumar K., VázquezHuerta G., Castellanos A. R., Varaldo H. M., SolorzaFeria O., *Int. J. Electrochem. Sci.* 7 (2012) 5491.
32. Ahmad Monshib A., Foroughi M.R., Monshi M. R., *World Journal of Nano Science and Engineering.* 2 (2012) 154.
33. Vishwanathan B., Indra P., Neel., Varadarajan T.K., *Catal Surv Asia.* 13 (2009) 166.
34. Sadezky A., Muckenhuber H., Grothe H., Niessner R., Poschl U., *Carbon.* 43 (2005) 1735.
35. Yuana X., Yuana D., Zenga F., Zoua W., Tzorbatzogloub F., Tsiakarasb P., Wang Y., *Appl. Catal., B.Environ.* 129 (2013) 370.
36. Saka C., *J. Anal. Appl. Pyrolysis*. 95 (2012) 23.
37.Britto. O.S.M., Andrade H.M., Soares L.F., Azevedo R.P., *J. Hazard. Mater.* 174 (2010) 85.
38. Namasivayam C., Sangeetha D., *J.Chem.Tech.* 12 (2005) 514.
 39. Shanthi T., Manonmani S., Smitha T., *J .Hazard. Mater*. 179 (2010) 180.

40. Langmuir I., *J. Am. Chem. Soc.* 40 (1918) 1361.
41. Gercel O., Gercel H.F., Koparal A.S., Ogutveren U.B., *J .Hazard.mater*. 160 (2008) 671.
42. Freundlich, H., *J. Z Phys. Chem.* 57 (1906) 385..
43. Mittal A., Mittal J., Malviya A., Gupta V.K., *J.Colloid Interface Sci*. 344 (2010) 502.
44. Mark Daniel G., de Luna., Edgar,D., Flores ., Divine Angela D., Genuino ., Cybelle M., Futalan , Wanc
     M., *J.Taiwan Inst Chem Eng.*44 (2013) 651.
45. Lagergren, S., *Handlingar*. 24 (1898)1.
 46. Panda G.C., Das S.K., Guha., *J. Hazard. Mater.* 164 (2009) 377.
 47. Weng H., Lin Y.T., Treng T.W., *J. Hazard .Mater.* 170 (2009) 421.
48. MohdSalleh M.A., Mahmoud D.K., Karim W.A., Idris A., *Desalination.* 280 (2010) 9.
49. Jain S., Jayaram R.V., *Desalination* 250 (2010) 923.
50. Kadirvelu K., Kavipriya M., Karthika C., Radhika M., Vennilamani N., Pattabhi S., *Bioresour Technol.*
      87 (2003)130.
51. Kannan N., Sundaram M.M., *Dyes and Pigments.* 51(2001) 39.
52. Hamdi M.H., Ashraf A., El-Sayed., *J.Hazard.Mater.* 168 (2009) 1079.
53. Leechart P., Nakbanpote W., Thiravetyan P., *J.Environ. Manage.* 90 (2009) 918.

(2015) ; http://www.jmaterenvironsci.com